*Fibers and Polymers* 2013, Vol.14, No.9, 1526-1534 DOI 10.1007/s12221-013-1526-0

# Morphological Aspects of Polymer Fiber Mats Obtained by Air Flow Rotary-jet Spinning

**Tudorel Bălău Mîndru, Leonard Ignat[1]*, Iulia Bălău Mîndru, and Mariana Pinteala[1]**

*Faculty of Textile Leather and Industrial Management, "Gh. Asachi" Technical University, Iasi 700050, Romania*
*[1]Centre of Advanced Research in Bionanoconjugates and Biopolymers, "Petru Poni" Institute of Macromolecular Chemistry, Iasi 700487, Romania*

(Received December 11, 2012; Accepted March 3, 2013)

**Abstract:** Fiber mats were obtained by using a modified rotary-jet spinning system, which allows a forced air flow produced by an air compressor to interfere with the polymer jets. The main focus of current studies rely on the range of morphological and dimensional characteristics of fibers that may be expected when using this new technical setup of a rotary-jet based spinning system. In fact, this work represents a proof of concept study regarding the potential of an air flow modified rotary-jet spinning for obtaining continuous fibers and nonwoven mats. The morphological examinations by scanning electron microscopy were proved the efficiency of this technique on obtaining relative homogeneous fiber mats from different raw compositions of pure and admixed, natural and synthetic polymers with different molecular masses and polydispersity degrees, like gelatin, polyurethane, and poly (vinyl chloride). The feasibility of air flow rotary-jet spinning was also tested for simultaneous independent deposition of mixed fiber mats from solutions of two polymers made in different solvents, and it was found that by carefully selecting the ratio of polymers through spinnerets number, this technique could be successfully used even in difficult solvent conditions otherwise incompatible with traditional spinning techniques. The distribution of fiber diameters was varying between nanometer scales (100-700 nm) in the case of pure polyurethane and micrometer ranges (2-12 $\mu$m) for gelatin-polyurethane mixed mats, which are convenient for various applications, from dressings and scaffolding to different filter systems. Besides the already known advantages of rotary-jet versus electrospinning, the air flow allows the control of solvent evaporation, extending the applicative range of this technique.

**Keywords:** Morphology, Fiber mats, Rotary-jet spinning, Centrifugal effect

## Introduction

Micro and nanofibers represent special categories of fibrous media with various applications in coatings, batteries, sensors, filter systems, drug delivery systems, tissue engineering, and scaffolding [1-3]. Fibers with diameters scaled up from tenths of nanometers to a couple of microns, originated from natural or synthetic polymers, are currently made by techniques mainly based on template synthesis, phase separation, self-assembly, drawing nozzle spinning, and electrospinning [4,5].

Electrospinning consists in applying a voltage of about 0.5 to 50 kV to a polymer solution made in polar solvents through a syringe nozzle, and has been proven so far as one of the attractive methods of making fibrous materials [6-8]. The polymer solution contained in syringe is delivered to the nozzle with a controllable speed provided by an automatic pump. According to the electrospinning principle, when the electrical forces overcome the surface tension of the solution, an electrically charged jet is ejected. As solvent evaporates, the resulting charged fibers are directed by electrical forces to a collector and deposited in different forms like sheets and rolls [9].

Although this technique has become relative common and frequently used, it suffer from a series of issues i.e. high electricity consumption and special protective measures due to the high voltage requirements, reduced deposition rates, low polymer concentrations, unstable jet flowing accompanied by variable and frequent breaking filaments [10]. Many efforts have been made to achieve significant improvements in the electrospinning techniques by modifying the traditional setups and working parameters. Recent successfully attempts [11-13] have conducted for example to an increase in productivity and cover area, and to finer and more even distributed fiber mats, by changing the nozzles configuration, co-axial deposition with salt solutions, or multi-jet electrospinning setups.

However, an easy way to surpass some basic electrospinning inconveniences consists in the use of the new rotary-jet spinning technique, which makes appeal to the centrifugal or rotational effect for obtaining nanofiber materials [14,15]. For example, the rotary-jet spinning needs only ordinary voltages (up to 230 V) and works at speeds up to 100 times faster, increasing the process efficiency. Another important advantage consists in the opportunity to work not only with polar solvents and dilute solutions, but with a wide range of solvents and concentrations, and even with polymer melts [16].

In rotary-jet spinning the polymer melt or solution is supplied to a spinning head fitted with nozzles and positioned on the axis of a centrifuge that could operates at working speeds between 3000 and 20000 rpm [16,17]. The liquid-state material is ejected through the head spinning nozzles due to the action of centrifugal force, while the rapid flowing of the surrounding air ensures the solvent evaporation,

*Corresponding author: lignat@icmpp.ro

respective the cooling of melts, conducting to nanofiber formation and consolidation. A key element during the process consists in finding the optimum balance between the speed of evaporation or cooling and solid filament formation [18]. The resulting nanofibers could be deposited on non-adherent supports of different geometries (i.e. planar, cylindrical, and conical). Both polymers and solvents may be used in pure forms or in different mixtures.

The way of deposition and final morphology depend on the polymer type and concentration, viscosity, temperature, as well as on processing parameters that are specific to the rotary-jet apparatus (working speed, spinning nozzles number and geometries, spinning head diameter and geometry) [10].

It was reported [19] that fiber matrices formation during rotary-jet spinning occurs in three main stages: jet initiation, elongation, and solvent evaporation. The jet elongation until reaching the support should be very well correlated with solvent evaporation in order to obtain fiber webs with appropriate and reproducible morphologies. As consequence, the solvent boiling temperature and vapor pressure, the speed and type of drying gaseous flow (air, nitrogen), together with the distance between nozzles and collector are important factors in controlling and adjusting the size, orientation and uniformity of fibrous media. Furthermore, if the rotational speed of the spinning head surpasses a critical threshold velocity, which is specific to a given fluid composition, the jet tend to be fragmented, conducting to irregularly deposits composed from broken fibers. On the contrary, when the head spins at too low speeds the fiber tend to unevenly increase in diameter and agglomerate with droplets formation. Such droplets also appear at jet initiation stage when the high vapor pressures of the solvent have been associated with an increased surface tension of the fluid.

All the above mentioned parameters simultaneously influence the formation of final fiber matrices, making very difficult the modeling of rotary-jet spinning processes. In this work, we have investigated the morphology of fibers obtained in a modified, home-made rotary-jet spinning apparatus, by using different raw compositions of pure and mixed, natural and synthetic polymers. The main improvements added to the apparatus as compared with the previously reported ones consist in the modulation of solvent evaporation by the insertion of a cooling/heating gaseous flow, and solvent vapor evacuation from spinning environment through a exhauster. Other parameters that can be regulated include the solution feeding mode, rotational speed, spinning head and nozzles diameters, as well as the distances from head axis and nozzle tip to the collecting surface.

## Materials and Method

### Materials

Poly (vinyl chloride) polymer (PVC; Mw~230,000) and polyethylene glycol (PEG; Mw~2,000) were purchased from Sigma-Aldrich, whereas the chitosan (Mw~200,000) and gelatin type B granules (100 bloom) were obtained from Fisher Scientific. The polyurethane polymer (PU; Mw~100,000) was synthesized in our laboratory by the two-stage polyaddition of 4,4'-diphenylmethane diisocyanate, poly (butylene adipate) and 1.4 butanediol in dimethylformamide (DMF), according to a previously reported procedure [20], purified by three successive precipitations in water and dried to constant weight. All other chemical reagents were of analytical grade and used as received from Sigma-Aldrich, Merck and Scharlau Chemie.

### Preparation of the Spinning Solutions

The polymer solutions were made in such concentrations to obtain viscosities within the optimum range of the experimental setup of our rotary-jet spinning apparatus. Before solvation in the appropriate solvents, all polymers were conditioned in a vacuum oven at 40 °C for 24 hours. The freshly prepared solutions were placed in sealed flasks, stirred at room temperature for at least 3 hours, until complete solving of polymers, and subsequently filtered through a glass wool filter to remove any eventual impurity or inhomogeneity. The apparent viscosity of polymer solutions, $\eta_a$, was determined at room temperature (25±0.1 °C) by using a Nahita Rotary Viscometer, in agreement with the ISO-3219:1993 standard specifications.

The solvents used and final polymer concentrations, together with the apparent viscosities of resulting solutions are summarized in the Table 1. Besides the pure polymer solutions, blends were also prepared by mixing at room temperature the solutions of chitosan and PEG (each of 4 % w/v final concentrations) with gelatin (30 % w/v) in 4:1 formic acid: acetic acid solvent mixture ($\eta_a$=1100 cp).

### Rotary-jet Spinning of Micro- and Nanofibers

The system used for obtaining polymer fibers by centrifugal effect was made in our laboratory and is schematically illustrated in Figure 1. It is basically composed of a thermo-stated spinning chamber that affords operations like polymer fluid supply, gaseous exchange, vapor exhausting, and surrounds

**Table 1.** Parameters of polymer solutions used in rotary-jet spinning experiments

| Polymer type | Solvents and volume ratio | Concentration (w/v %) | Apparent viscosity [$\eta_a$] (cp) |
|---|---|---|---|
| PVC | CHN : DMF (1:1) | 16 | 820 |
| PU | DMF | 20 | 870 |
| G | FA : AA (4:1) | 30 | 930 |
| G | FA : AA (4:1) | 40 | 1200 |

where, PVC: poly (vinyl chloride), PU: polyurethane, G: gelatin; CHN: cyclohexanone, DMF: dimethylformamide, FA: formic acid, and AA: acetic acid.

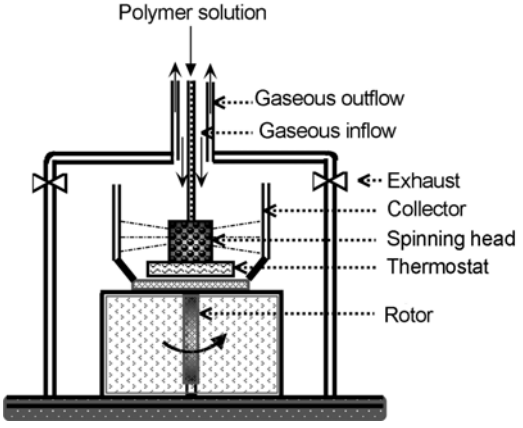


**Figure 1.** Schematic configuration of the rotary-jet spinning system.

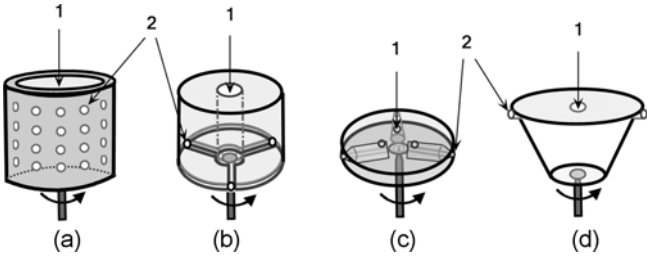


**Figure 2.** Spinning heads with various geometries; (a) cylindrical with multiple nozzles, (b) cylindrical with channeled nozzles, (c) cylindrical with individual spinnerets for discontinuous processes, and (d) truncated cone shaped with radial nozzles (1: polymer solution feeding, 2: spinning holes).

the moving parts of the rotary-jet equipment (rotor, spinning head) and polymer fiber collector. The rotational speed, air flow and temperature, polymer dosage, and exhaust blowers are externally controlled.

Different spinning heads with various geometries were tested to obtain a preliminary evaluation of fibers deposition (Figure 2).

Discontinuous depositions were carried out by using a cylindrical spin head provided with individual spinnerets having limited storage capacities for polymer solutions (Figure 2(c)). This procedure was applied for obtaining mixed fibers from two polymer solutions made in different solvents, in particular gelatin (30 % w/v) and PU (20 % w/v). Two spinnerets were used to obtain a 1:1 ratio between mixed polymer fibers (GPU1), and three spinnerets for G/PU ratios of 1:2 (GPU2) and 2:1 (GPU3). In all other cases, a continuous deposition was achieved by supplying the polymer solutions, with an appropriate flow controlled by a peristaltic pump, from an external reservoir to the center of the spinning head through a central pipe (Figures 2(a), (b) and (d)). Besides the pure polymer solutions (PVC, PU, G30%, and G40%), the blend of G30% with chitosan (4% w/v) and polyethylene glycol (4 % w/v) in 4:1 formic acid: acetic acid solvent mixture (GCP) was also used for fiber deposition in the continuous mode.

**Table 2.** Parameters for the rotary-jet spinning of polymer solutions

| Polymer solutions | Rotational speed (rpm) | Air flow temperature ($^{o}$C) | Spinning nozzle diameter ($\mu$m) |
|---|---|---|---|
| PVC | 3000 | 40 | 300 |
| PU | 3500 | 40 | 300 |
| G30 | 3000 | 25 | 300 |
| G40 | 3000 | 25 | 300 |
| GPU1 | 2800 | 25 | 200 |
| GPU2 | 2800 | 25 | 200 |
| GPU3 | 2800 | 25 | 200 |
| GCP | 3500 | 25 | 300 |

where, PVC: poly (vinyl chloride), PU: polyurethane, G: gelatin, GPU: gelatin/polyurethane mixtures, and GCP: gelatin/chitosan/polyethylene glycol mixtures.

The distances between collecting surfaces and spinning axes, respective nozzles tips, were set to 19 cm and 11 cm for all experiments, whereas the diameters of horizontal tubes or spinnerets (Figures 2(b) and (c)) were regulated to be of 2.54 cm. A constant air flow of 30L per second was assured by an external air compressor, model Fini-Amico 25. The air flow circulation inside spinning chamber is also influenced by centrifugal effect. The other technological conditions and parameters applied during the modified rotary-jet spinning of polymer micro- and nanofibers are summarized in the Table 2.

### Characterization

The morphological properties of polymer fibers obtained through the current modified rotary-jet spinning process were examined using a Vega-II Tescan scanning electron microscope (SEM, Czech Republic), and Atlas Tescan software for image analysis. Prior to SEM investigation, all samples were sputtered with gold. An accelerating voltage of 30 kV was used for image acquisition. The SEM images were furthermore analyzed by using the ImageJ software (NIH, USA) in order to have a better approximation of the fiber thickness and their diameters distribution.

## Results and Discussion

The rotary-jet spinning based on centrifugal effect represents one of the most recent and efficient ways to obtain fibers with diameters varies from tens of nanometers to a couple of micrometers. Despite it's already proved advantages over other methods like electrospinning, the rotary-jet spinning processes are susceptible to further modifications in order to add even more improvements, one of such modification being reported in the present work. Moreover, the use of

rotary-jet spinning in obtaining thin fiber mats evolved merely in the past couple of years, the aforementioned reports being some of the very few founded in the literature survey. The main difference of our proposed system as compared with other rotary-jet spinning equipments consists in the fact that it allows the control of solvent evaporation by the use of a cooling/heating gaseous flow in the spinning chamber that surrounds the rotating active part. Also, the gaseous flow may be evacuated through an exhaust blower. Besides the surface tension of polymer solution and solvent vapor pressure, the evaporation speed and medium saturation with vapors represents very important parameters in the formation of continuous, low diameter fibers and uniform matrices and could be controlled by varying the flow rate and temperature of gaseous environment. The influences of other processing variables like distance from the centrifugal axis to the collector, rotational speed, spinning head and nozzles diameters were preliminary evaluated and adjusted to obtain the best performance in rapport with each tested polymer solution.

Different geometries of the collecting supports may be used for fiber deposition, regardless of the types of spinning head and polymer solutions involved, as can be seen from the examples illustrated in Figure 3.

An important factor for the successful rotational spinning of any synthetic or natural polymer consists in the preparation of solutions with adequate concentrations, rheological properties and stability. We have previously found that a mixture of formic and acetic acid in 4:1 volumetric ratio enhances the gelatin solvability, lowers the viscosity, and provides a good stability and homogeneity of the resulting solutions [21].

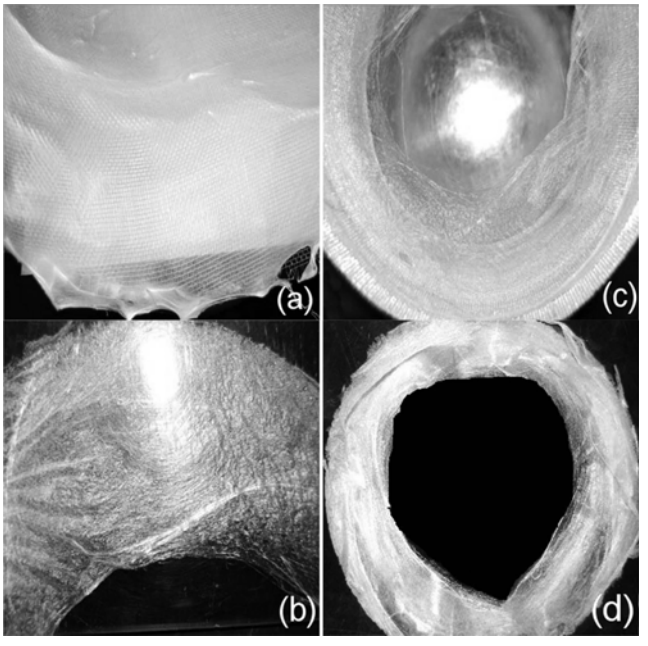


**Figure 3.** Optical photographs of fiber mats collected from planar (a, b) and circular (c, d) supports.

This partial substitution of formic acid with acetic acid favors the formation of dynamic supramolecular associations of gelatin molecules by temporary hydrogen bonds in a way that keep the solution structurally stable and increase its apparent viscosity. Preliminary tests were carried out with each polymer solution in order to establish the most appropriate solvents and concentrations domains for a successful formation of fiber mats (Table 1).

**Surface Morphology and Fiber Diameters**

The main focus of current works rely on the range of morphological and dimensional characteristics of fibers that may be expected when using this new technical setup of a rotary-jet based spinning system. For this reason, SEM images were taken from the surface of different fiber mats obtained from gelatin, PU, and PVC, as well as from the simultaneous spinning of gelatin and PU solutions. These polymers were chosen to show the potential of our modified rotary-jet technique since they are commonly used and, on the other hand, are quite different as origin, structure, rheology, solubility, elasticity, stiffness, and other specific properties. Preliminary tests were made for adjusting the characteristics of polymer solutions and dynamic parameters, with the aim of obtaining appropriate fiber mats in conditions of better reproducibility, lower rotational speed and less used solvent in comparison with the case of a typical technique [10,17]. As mentioned before (Figure 2(b), Table 2), the constructive parameters of rotary-jet apparatus were mostly the same during the experiments, with the exception of the individual spinnerets with narrower tips (Figure 2(c), Table 2) which were used for simultaneous deposition of fibers from different polymer solutions. In these conditions, the best performances were obtained for polymer solutions having apparent viscosities between about 800 and 1200 cps (Table 1), which correspond to variations in polymer concentrations ranging from 16 % (PVC) to 40 % (gelatin), and rotational speeds as low as 2800-3500 rpm. The spinning of PU and PVC solutions was made at slightly higher air flow temperature (40 $^{o}$C) in order to partially compensate the low vapor pressure of solvents used. The common tendencies to filaments winding around the spinning head and spinneret clogging observed during typical spinning techniques could be also noticed in the current embodiment, and are favored by increasing the air flow temperature. These issues were limited by an appropriate correlation between the rheological behavior of polymer solutions and working conditions like rotational speed, air flow and temperature. The use of channeled nozzles with geometries and surfaces that promote the polymer flow and self-cleaning behavior is also important for clogging prevention before the effective air flow spinning. Nevertheless, extensive experimental works should be done to optimize the rheological and process parameters for each particular case of spinning solution. It must be noted that while proper optimization studies are very complex and still

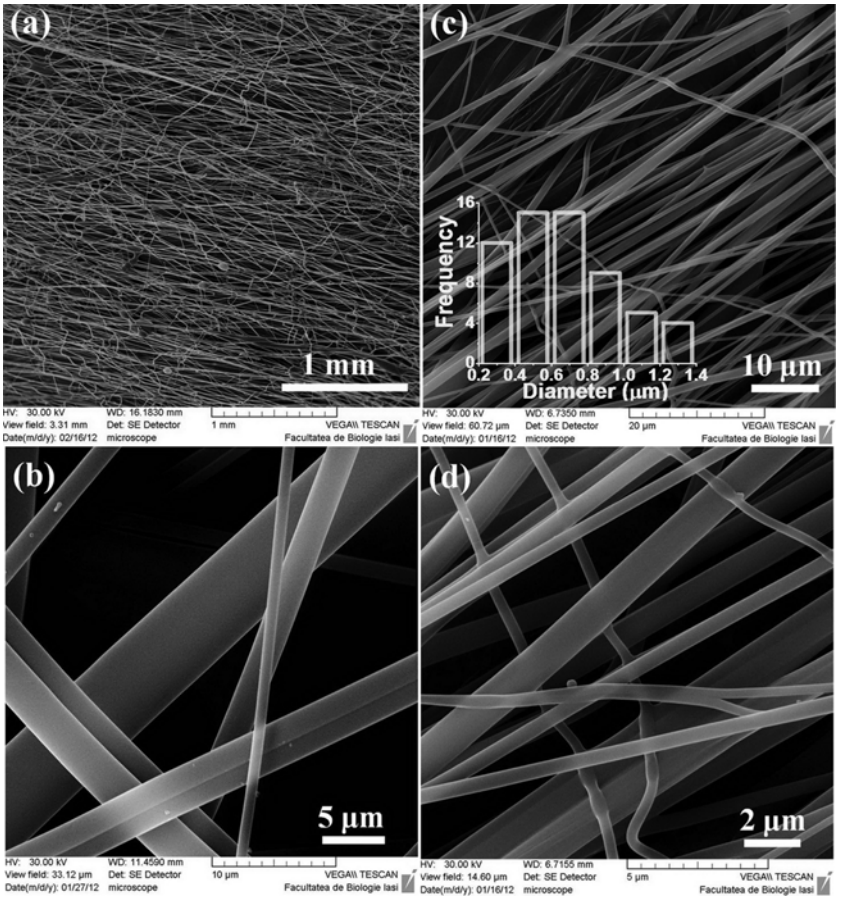


**Figure 4.** SEM images of gelatin fiber mats at different scales: G40% (a, b) and G30% (c, d).

underway, the parameters presented here being chosen to illustrate the potential of our practical concept of rotary-jet spinning for obtaining thin fibers and depositing them under the form of porous membranes.

At a first glance, the SEM images have revealed in all cases the formation of a highly porous matrix constructed from entangled and interlocked fibers disposed in more or less random directions (Figures 4-7). Also, unlike the results of a typical technique, fibers obtained here are very smooth and coalescence is partially avoided due to the continuous air flow provided during deposition. However, the fiber diameter distribution is still relative large and non-uniform, in agreement with the results of traditional spinning techniques [17,22]. In addition, the general presentation of deposition mats, and fibers diameters that generally varies between around 100 nm and several micrometers, are appropriate with those just reported [16] in the case of rotary-jet spinning of poly(butylene terephthalate) melts at very high speeds and temperatures ($1\text{-}5\times10^4$ rpm; ~ 300 °C).

The morphology of gelatin mats, as illustrated in Figure 4(a), is the results of a combination between high numbers of relatively straight, loosely oriented fibers and bunches of random, irregular and generally thinner fibers, together with scattered beads and coalescent segments.

The simultaneous presence of beading and coalescence processes, although limited, is due to the high polydispersity of gelatin molecular weights. In fact, the average molecular mass of gelatin with a low bloom number of 100 is around 25,000, but its solutions may contain significant fractions of chains with molecular weights up to several times higher and lower than the average. On the other hand, it is known that the molecular weight of polymers greatly affects the optimum concentration range for spinning processes in an inverse proportional way [23]. As a consequence, the optimum concentration range for a highly polydisperse solution is difficult to estimate and supposes the coexistence of beads given by the lowest molecular weight fractions with coalescent segments determined by the highest ones. Moreover, as can be observed by comparing the SEM images from Figures 4(b) and (d), the decrease in gelatin concentration from 40 % to 30 % conducts to an important reduction of fiber diameters from micrometer (~1-5 $\mu$m) to predominant sub-micrometer domain (~0.2-1.4 $\mu$m), without changing the overall pattern of resulting matrices (Figure 4(c)). In all instances, the resulting fiber surfaces are very smooth and only limited or no stickiness may be observed when

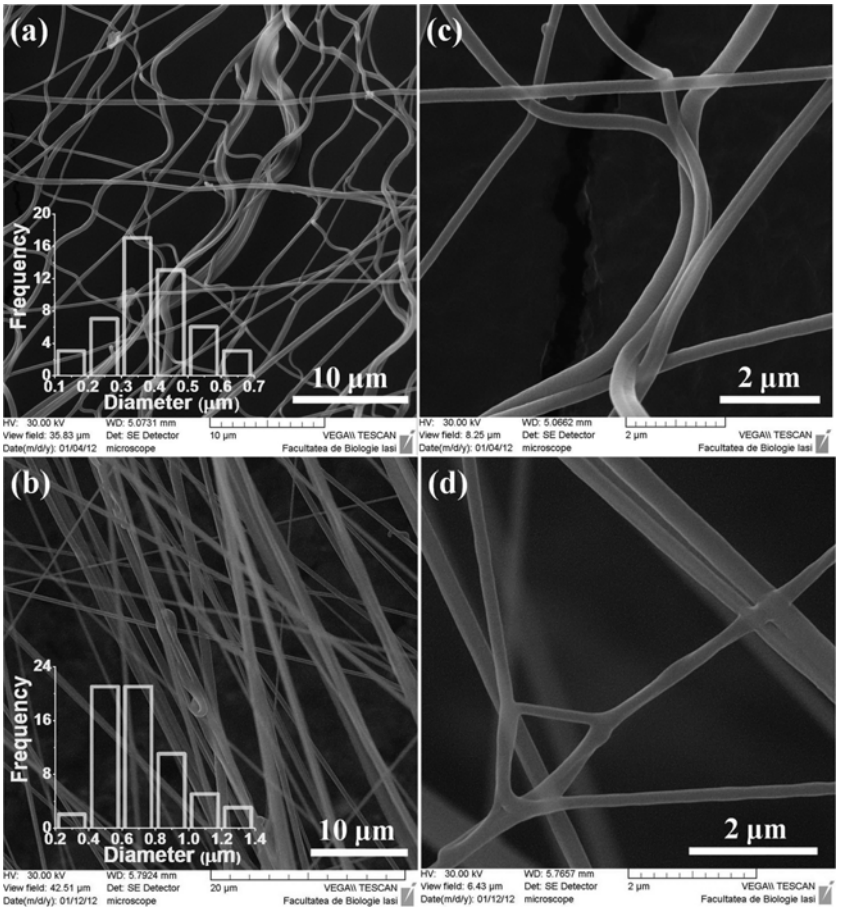


**Figure 5.** SEM images and diameter distributions of fiber mats made of (a) PU, and (b) PVC. Close views of PU and PVC fibers are shown on the right (c, d).

superimposed. The thinnest and irregular fibers results due to the breakings in polymer jets generated by normal occurring jet instabilities and favored by the air flow impact. After breaking, fibers are also supplementary stretched and randomly deposited under the action of air flow.

Unlike gelatin, the PU and PVC were synthetic polymers with much lower polydispersity and higher molecular weights, which have determined narrower and lower levels of working concentrations (Table 1). The apparent viscosities were also a bit lower than those of gelatin solutions, and in the case of PU a small increase in rotational speed from 3000 to 3500 rpm was needed to preserve a loosely porous structure of the mats. The striking difference of resulting mats observed in Figure 5 is not due to the intrinsic flexibility of elastomeric PU as compared with the stiff, plastic PVC, but to the difficult evaporation of solvent even in a 40 $^{o}$C continuous air flow caused by extensive hydrogen bonding arising between DMF and PU chains. The PU lower molecular weight than PVC, DMF low vapor pressure, and air flow pressure also favors the extension of bending instabilities and formation of the wavy, curly non-woven nets presented in Figures 5(a) and (c). The fiber diameters (Figure 5(a), lower inset) show an almost Gaussian distribution exclusively placed in the nanometer range (100-700 nm), values about two times lowers than those obtained for G30%.

As opposed to PU, the PVC fibers are straight and forms matrices with characteristics comparable with those made of gelatin, despite the use of a low vapor pressure solvent mixture. The PVC fiber diameters (Figure 5(b), lower inset) present a somewhat tighten distribution than that of G30%, but cover the same range. However, the fiber surfaces tend to be sometimes lightly non-uniform and sparse coalescence of superposed fibers occurs, suggesting that PVC working solution is close to the upper limit of optimum concentration.

In order to furthermore investigate the effect of polydispersity on the quality of resulting polymer matrices, a solution of G30% was mixed with compounds having much higher Mw (chitosan) and respective lower Mw (PEG), the later additive having also a compatibilizer role. The resulting blend was spun in the same conditions as gelatin, except the rotational speed that was gentle increased to 3500 rpm in an attempt to increase the homogeneity and reduce the fiber diameters. As

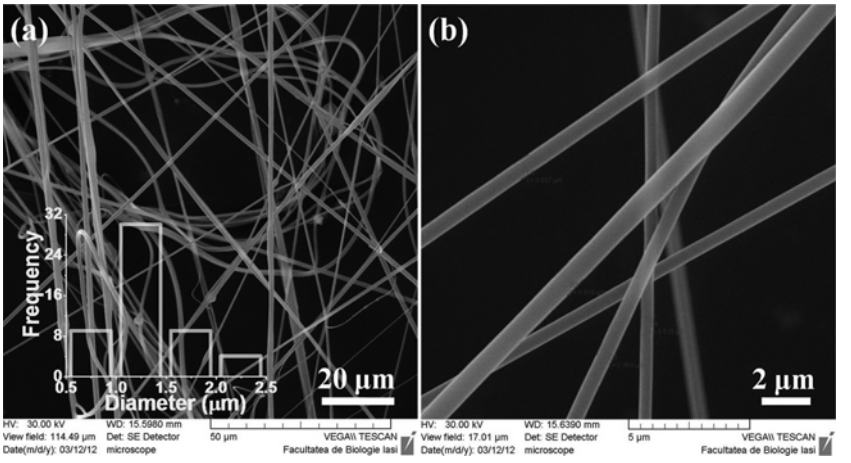


**Figure 6.** SEM images and diameter distributions of fiber mats spun from GCP pre-blended solutions.

expected, the fiber mats have poorer presentations (Figure 6) comparative with those obtained from gelatin only (low homogeneity reflected by larger pores combined with zonal agglomerations, fibers with random deposition, orientation, and straightness). In addition, the distribution of fiber diameters is shifted upward, mostly between 0.5 and 2.5 μm (Figure 6(a), lower inset).

The lower homogeneity of fiber mats obtained from mixed solutions of highly polydisperse polymers reduces their applicative potential. A solution to overcome this issue consists in the sequential, discontinuous deposition of layers from polymer fractions with lower polydispersity, but such procedure is time consuming and modifies the structural homogeneity across the depth of the mats. Other possibility is based on simultaneous and independent deposition of two or more distinct polymer solutions through individual spinnerets. From applicative point of view, it was very interesting to test the feasibility of our technique for deposition of mixed fiber mats from solutions of two polymers made in different solvents. This procedure was applied in particular for G30% and PU solutions made in solvents with very different vapor pressures (Table 1), each of them loaded in one or two spinnerets (Figure 2(c)) for obtaining G/PU ratios of 1:1 (GPU1), 1:2 (GPU2), and 2:1 (GPU3).

The simultaneous presence of DMF on one hand and acetic and formic acid on the other hand greatly interferes with fiber spinning. For example, the gelatin solvents have higher vapor pressures and lower vapor densities than DMF and tend to saturate the air flow, inhibiting the DMF evaporation. They are also miscible with DMF and non-solvents for PU, so could generate random, local abnormal increases in viscosities, which in turn determines irregular diameters and shapes on the length of the same fiber and intensifies the fibers coalescence. Moreover, the PU solvent produces the same effects on gelatin fibers. There is also an overall effect on increasing the fiber diameter distributions, as shown in Figures 7(a), (b), and (c), even in conditions of using nozzle diameters of 200 μm instead 300 μm. In addition, it can be clearly seen that all obtained mats more resemble those of pure gelatin, while the wavy net behavior of the PU component is not expressed at all as result of the simultaneous spinning of DMF, acetic and formic acid polymer solutions.

Fiber diameters were generally in the range of 2 to 12 μm in all cases, GPU1 having the best distribution centered at about 7 μm. It must be mentioned that well outside the main domain investigated using Image J software were observed agglutinated fiber parts (Figure 7(c)) and residual sparse fibers in the nanometer range (Figures 7(a) and 7(c)). These fibers show diameters of about 100-200 nm and can be better viewed at higher magnification (Figures 7(d) and 7(f)). The thin fibers formation is related to the G/PU ratio, and in particular to the proportion between gelatin solvents and DMF, rising from a negligible amount for GPU2 to about 20 % for GPU3. Furthermore, the solvents used are miscible, but gelatin solubility in DMF is very low whereas the others may precipitate the polyurethanes. As a consequence, the resulting vapors interfere with the viscosity and stretching behavior of extruded jet. Obviously, these interferences are enhanced by increasing the amount of the higher volatile solvents. Thus, the process seems to involve the different stretching of filaments in the air flow enriched by an increased amount of vapors coming from the higher volatile solvents [10] rather than subsidiary jets formation and backbone emitted nanofibers observed at the electrospinning of complex mixtures [7,24]. This supposition is also supported by the results obtained at gelatin and polyurethane non-mixed mats (Figures 4(c) and 5(a)), where fibers distributions include fractions of relative similar diameters. The solvents interference may also compromise the jets stability, inducing coalescence and bead formation. Both effects are clearly shown in Figure 7, where the G/PU ratio of 2:1 (GPU3) (Figures 7(c) and 7(f)) was led to the lowest quality mats, characterized by relative frequent coalescence and a high

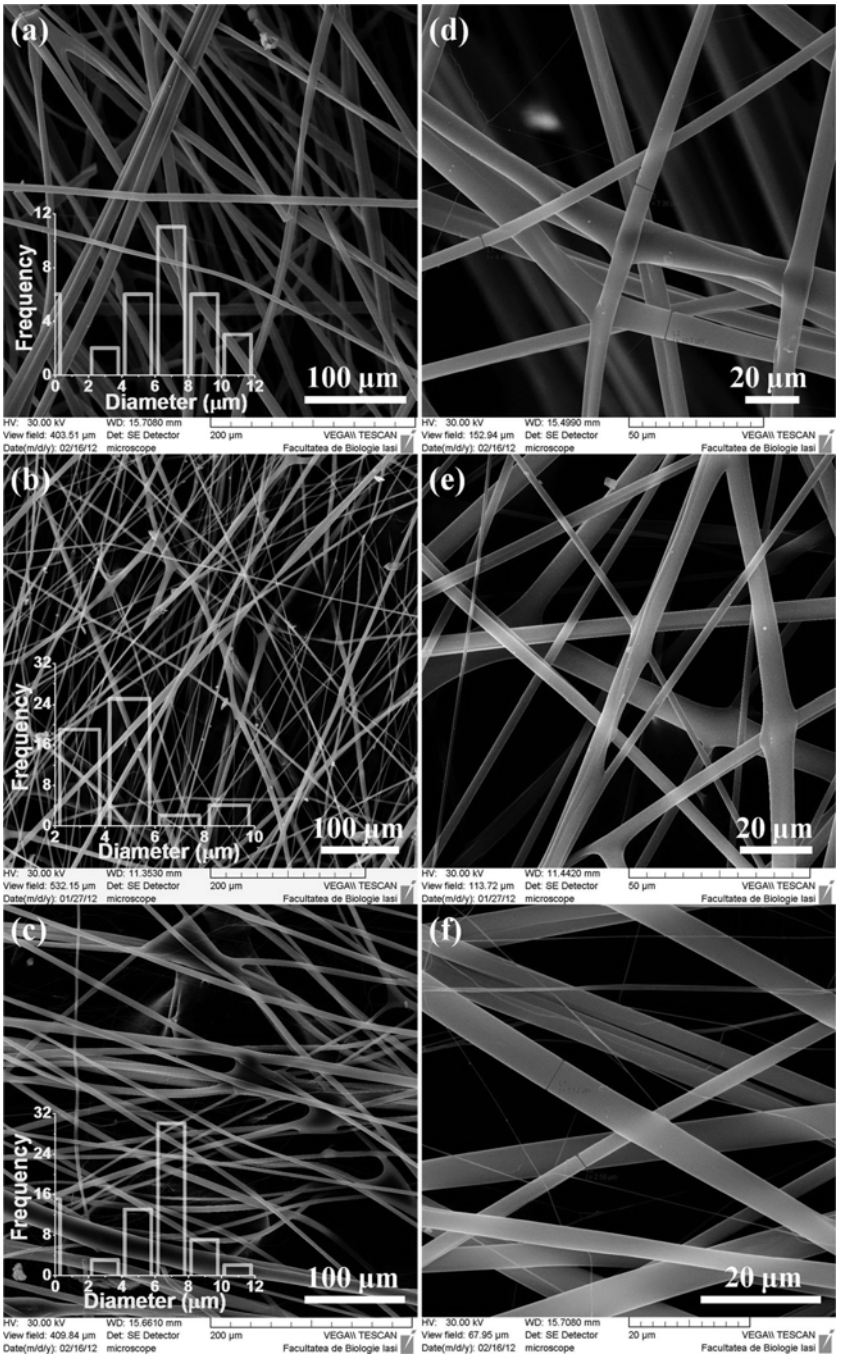


**Figure 7.** SEM images and diameter distributions of mixed fiber mats made of (a) GPU1, (b) GPU2, and (c) GPU3. Close views of GPU1-GPU3 mixed fibers are shown on the right (d-f).

proportion of very thin fibers. However, the formation of polymer fiber matrices was accomplished in all cases, so the air flow rotary-jet spinning was proved to be a viable solution for mixed fiber mats deposition.

By carefully selecting the ratio of polymers through spinnerets number, the air flow rotary-jet spinning could be successfully used to produce mixed fiber mats even in difficult solvent conditions that are incompatible with traditional spinning techniques. This technique provides a higher flexibility in choosing the raw spinning solution, processing parameters, and final product characteristics. Therefore it affords the production of various non-woven textiles, responsive materials based on one or several polymers, blends and composites matrices, which could be more

reliable than current fiber mats in applications like filtering devices, covering membranes, dressings, and scaffolds.

## Conclusion

This work represents a proof of concept study regarding the potential of an air flow modified rotary-jet spinning for obtaining continuous fibers and nonwoven mats. Besides the ordinary advantages of rotary-jet versus conventional electrospinning, the air flow allows the control of solvent evaporation, extending the applicative range of this technique. The morphological examinations were proved the efficiency of this technique on obtaining relative homogeneous fiber mats from solutions of natural and synthetic polymers with different molecular masses and polydispersity degrees. Moreover, the simultaneous independent spinning of polymer solutions affords the production of appropriate mixed fiber mats from at least two polymer solutions made in different solvents. The distribution of fiber diameters varies between nanometer scales (100-700 nm) in the case of PU and micrometer ranges (2-12 $\mu$m) for GPU1-GPU3 mixed mats, which are convenient for various applications, from dressings and cell supports to different filter systems. The fibers morphology and mats homogeneity depends on a wide range of spinning solution characteristics (i.e. polymer type, molecular weight, polydispersity, concentration, viscosity, solvent vapor pressure) and operational parameters (i.e. rotational speed, spinning head configuration, nozzles diameter and geometry, distance to collector, temperature). Further investigations and appropriate modeling and simulations are currently undertaken to elucidate the complex interplay between these numerous factors and optimize the overall process.

## Acknowledgements

One of the authors (L. Ignat) acknowledges the financial support of European Social Fund – "Cristofor I. Simionescu" Postdoctoral Fellowship Programme (ID POSDRU/89/1.5/S/55216), Sectoral Operational Programme Human Resources Development 2007-2013.

## References

1. A. L. Andrady, "Science and Technology of Polymer Nanofibers", pp.183-248, Wiley-Interscience, New York, 2008.
2. W.-J. Li, C. T. Laurencin, E. J. Caterson, R. S. Tuan, and F. K. Ko, *J. Biomed. Mater. Res.*, **60**, 613 (2002).
3. J. A. Matthews, G. E. Wnek, D. G. Simpson, and G. L. Bowlin, *Biomacromolecules*, **3**, 232 (2002).
4. S. Ramakrishna, K. Fujihara, W.-E. Teo, T.-C. Lim, and Z. Ma, "An Introduction to Electrospinning and Nanofibers", pp.1-17, World Scientific Publishing, Ton Tuck Link, Singapore, 2005.
5. R. Nayak, R. Padhye, I. L. Kyratzis, Y. B. Truong, and L. Arnold, *Text. Res. J.*, **82**, 129 (2012).
6. D. R. Salem in "Nanofibers and Nanotechnology in Textiles" (P. J. Brown and K. Stevens Eds.), pp.3-21, Woodhead Publishing, Cambridge, 2007.
7. D.-G. Yu, J.-M. Yang, L. Li, P. Lu, and L.-M. Zhu, *Fiber. Polym.*, **13**, 450 (2012).
8. D.-G. Yu, G. R. Williams, L.-D. Gao, S. W. Annie Bligh, J.-H. Yang, and X. Wang, *Colloids Surf., A*, **396**, 161 (2012).
9. D. H. Reneker and A. L. Yarin, *Polymer*, **49**, 2387 (2008).
10. M. R. Badrossamay, H. A. McIlwee, J. A. Goss, and K. K. Parker, *Nano Lett.*, **10**, 2257 (2010).
11. C. H. Park, C.-H. Kim, H. R. Pant, L. D. Tijing, M. H. Yu, Y. Kim, and C. S. Kim, *Text. Res. J.*, **83**, 311 (2013).
12. A. Varesano, R. A. Carletto, and G. Mazzuchetti, *J. Mater. Process. Technol.*, **209**, 5178 (2009).
13. D.-G. Yu, K. White, J.-H. Yang, X. Wang, W. Qian, and Y. Li, *Mater. Lett.*, **67**, 78 (2012).
14. K. K. Parker, M. R. Badrossamay, and J. A. Goss, *W. O. Patent*, 132636 (2010).
15. A. Fabbricante, J. S. Fabbricante, and T. J. Fabbricante, *U. S. Patent*, 7857608 (2010).
16. K. Shanmuganathan, Y. Fang, D. Y. Chou, S. Sparks, J. Hibbert, and C. J. Ellison, *ACS Macro Lett.*, **1**, 960 (2012).
17. R. T. Weitz, L. Harnau, S. Rauschenbach, M. Burghard, and K. Kern, *Nano Lett.,* **8**, 1187 (2008).
18. K. Sarkar, C. Gomez, S. Zambrano, M. Ramirez, E. de Hoyos, H. Vasquez, and K. Lozano, *Materials Today*, **13**, 12 (2010).
19. P. Mellado, H. A. McIlwee, M. R. Badrossamay, J. A. Goss, L. Mahadevan, and K. K. Parker, *Appl. Phys. Lett.*, **99**, 203107 (2011).
20. C. Ciobanu, M. Ungureanu, L. Ignat, D. Ungureanu, and V. I. Popa, *Ind. Crops Prod.*, **20**, 231 (2004).
21. V. Tura, F. Tofoleanu, I. Mangalagiu, T. Balau Mindru, F. Brinza, N. Sulitanu, I. Sandu, D. Raileanu, and C. Ionescu, *J. Optoelectron. Adv. M.*, **10**, 3505 (2008).
22. C.-H. Park, C.-H. Kim, L. D. Tijing, D.-H. Lee, M.-H. Yu, H. R. Pant, Y. Kim, and C. S. Kim, *Fiber. Polym.*, **13**, 339 (2012).
23. S.-P. Rwei and C.-C. Huang, *Fiber. Polym.*, **13**, 44 (2012).
24. H. R. Panta, P. Risal, C. H. Park, L. D. Tijing, Y. J. Jeong, and C. S. Kim, *Colloids Surf., B*, **102**, 152 (2013).